Biologically-Enhanced Removal of PCE from NAPL Source Zones

N A T H A N   C O P E   A N D   J O S E P H   B .   H U G H E S *

Department of Environmental Science and Engineering, Rice University, 6100 Main Street, Houston, Texas 77005-1892

The influence of dechlorinating microorganisms on PCE and its reduction products in a residual nonaqueous phase liquid (NAPL) source zone was investigated. Experiments were conducted in upflow columns containing glass beads (diameters 500–750 μm) contaminated with a residual NAPL consisting of tridecane and labeled ^{14}C-PCE. Three columns were inoculated with a mixed PCE-dechlorinating culture, that was fed electron donor (pyruvate) at concentrations of 25, 100, and 250 mM. Pyruvate was fermented in all columns with essentially no methanogenic activity. Comparisons between actively dechlorinating columns and abiotic-PCE columns demonstrated that dechlorination resulted in an increase in total PCE removal, up to a factor of 16 over dissolution. PCE was sequentially reduced to trichloroethene, *cis*-dichloroethene, and vinyl chloride without ethene formation over the experimental period in the two columns operated at the lower electron donor levels. Total chlorinated ethenes removal for the columns that retained dechlorinating populations was enhanced from 5.0 to 6.5 times over the removal that would have resulted from dissolution alone. The system fed the highest pyruvate levels, interestingly, lost dechlorinating activity early in the experiment.

Introduction

Tetrachloroethene (PCE) and trichloroethene (TCE) are two of the most prevalent contaminants in groundwater (*1, 2*). Their low aqueous solubility and miscibility in organic co-contaminants often lead to PCE and TCE contaminated sites characterized by the presence of nonaqueous phase liquid (NAPL) source zones that present unique remediation challenges (*3, 4*). Pump-and-treat systems alone have been ineffective in the remediation of NAPL source zones (*5*).

Microbial reductive dechlorination of PCE and TCE has been investigated for nearly two decades (*6–16*), typically focusing on the bioremediation of dissolved plumes (*17, 18*). Investigations into dechlorination-based source zone restoration have begun only recently (*19, 20*). Past efforts of source-zone remediation have been concerned with the potential toxicity of high contaminant concentrations on the microbial populations, but several studies have confirmed biological dechlorination occurring at aqueous saturation PCE concentrations and high concentrations of TCE (*16, 20–23*). Halorespiring organisms might actually have an advantage in environments of high PCE and TCE concentrations, such as NAPL source zones, where organisms normally competing with them for energy sources are not able to thrive (*20, 24–27*).

In NAPL source zones where dechlorination activity is not observed, the rate of chlorinated solvent removal is controlled by dissolution. Dechlorination can serve to increase observed dissolution rates by decreasing chlorinated ethene concentrations at the NAPL/aqueous interface, thereby increasing the overall mass-transfer rates into the aqueous phase (*28, 29*). The reduced chlorinated ethenes all have greater aqueous solubilities than PCE allowing for higher total aqueous chlorinated ethene concentrations. As described by Carr et al. (*19*), if dechlorination rates in source zones are sufficiently rapid, it may be possible to substantially reduce the longevity of the PCE component of the NAPL and minimize the time required for site restoration.

Partitioning of aqueous contaminants back into NAPL source zones presents a complicating factor in the analysis of how dechlorination processes effect source zone longevity. PCE dechlorination yields the reduced chlorinated ethenes, TCE, *cis*-dichloroethene (*cis*-DCE), and vinyl chloride (VC), which tend to partition back into the NAPL, causing temporal changes in NAPL composition and the concentration of total ethenes in the aqueous phase. Each of these dechlorination products partitions more readily to the aqueous phase than their parent compounds, increasing the flux of total ethenes from source zones. All of the chlorinated PCE reduction products are regulated contaminants themselves, which necessitates their complete removal from the source for remediation to be complete (*3*).

The objectives of the studies presented herein are to determine whether dechlorinating bacteria can reduce the time required to deplete the PCE fraction of a simulated NAPL source zone, to evaluate the effects of dechlorination on chlorinated ethene distribution between the NAPL and aqueous phase, and to examine the effect of electron donor concentration on chlorinated ethene removal rates. Experiments were conducted in upflow porous media columns containing a residual NAPL and an inoculum of PCE-dechlorinating enrichment culture. Results demonstrated that dechlorination could substantially reduce the longevity of PCE in NAPLs compared to dissolution alone, but results did not establish a clear link between electron donor feed concentration and observed dechlorination activity.

Materials and Methods

Chemicals. The following chemicals were obtained in liquid form: tetrachloroethene (99+%, Acros); ^{14}C-tetrachloroethene (100 μCi, Sigma); trichloroethene (99.5%, Acros); *cis*-dichloroethene (97%, Acros); 1,1,1-trichloroethane (99.5%, Aldrich); tridecane (99%, Sigma); pentane (HPLC grade, Acros); methanol (certified ACS, Fisher); and glacial acetic acid (ACS Reagent, Sigma). Gaseous chemicals obtained from Trigas included vinyl chloride (8%, balance N₂) and propane (99.95%). Ethene (99.5%) and methane (99%) were obtained from Scott Specialty Gases. Pyruvate (99+%) and propionate (99+%) were acquired as sodium salts from Sigma. Scintillation cocktail (Scinitsafe, Fisher) was used for ^{14}C measurements.

Nutrient Medium. Reagent-grade chemicals were used in the preparation of nutrient medium. The medium consisted of the following: 400 mg/L NH_4Cl, 400 mg/L KCl, 400 mg/L $MgCl_2 \cdot 6H_2O$, 140 mg/L KH_2PO_4, 25 mg/L $CaCl_2 \cdot 2H_2O$, 10 mg/L $(NaPO_3)_{16}$, 2.5 mg/L KI, 2.5 mg/L $CoCl_2 \cdot 6H_2O$, 0.5 mg/L $ZnCl_2$, 0.5 mg/L $MnCl_2 \cdot 4H_2O$, 0.5 mg/L H_3BO_3, 0.5 mg/L $NiCl_2 \cdot 6H_2O$, 0.5 mg/L $Na_2MoO_4 \cdot 2H_2O$, 0.5 mg/L NH_4VO_3, 200 mg/L yeast extract, pyruvate (ranging in

* Corresponding author phone: (713)348-5903; fax: (713)348-5203; e-mail: hughes@rice.edu. Corresponding address: Department of Environmental Science and Engineering, George R. Brown School of Engineering, Rice University, 6100 Main Street – MS 317, Houston, TX 77005-5903.
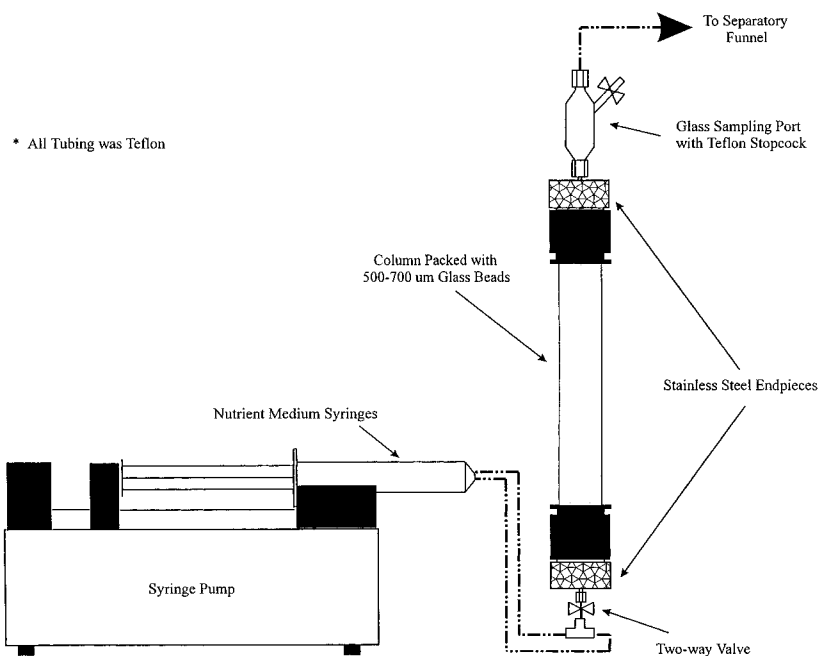
FIGURE 1. Schematic of columns used in experiments.

concentration from 2.75 mg/L to 27.51 mg/L), and NaHCO$_3$ as needed to buffer the systems (ranging in concentration from 3.0 to 5.5 g/L).

Analytical. Gas chromatography was used to determine the aqueous phase concentrations of all chlorinated ethenes and organic acids. Quantification of PCE and TCE concentrations was accomplished by extracting aqueous samples (150 μL) in pentane (5 mL) for injection (1 μL) into a gas chromatograph (Hewlett-Packard 5890) equipped with an electron capture detector (ECD). The GC was fitted with a VOCOL capillary column (60 m $\times$ 0.75 mm ID, 1.5 μm film; Supelco), and the temperatures of the oven, injection port, and detector were maintained at 100, 200, and 300 °C, respectively. Helium was the carrier gas (8 mL/min) and nitrogen was used as the auxiliary and anode purge gas (56 mL/min). Standards were prepared by adding known masses of PCE and TCE dissolved in methanol to vials containing pentane (5 mL) and deionized water (150 μL). All samples were spiked with an internal standard of 1,1,1-trichloroethane (final concentration of 415 mg/L) prior to the analysis. Nominal aqueous phase detection limits for PCE and TCE were 10 and 60 μg/L, respectively.

Headspace analysis was used to quantify methane, ethene, *cis*-DCE, and VC. Aqueous samples (5 mL) were added to serum bottles (70 mL) crimped with Teflon-lined butyl rubber septa. Propane (100 μL) was added as an internal standard prior to analysis. Each sample was allowed sufficient equilibration time, after which headspace samples (100 μL) were directly injected onto a GC (Hewlett-Packard 5890) equipped with a flame ionization detector (FID) and a packed column (6 ft $\times$ 1/8 in. OD) containing 60/80 Carbopack B/1% SP-1000 (Supelco). The operating parameters were as follows: 40 °C, hold 2 min., ramp at 20 °C/min. to 150 °C, ramp at 10 °C/min. to 200 °C, hold 10 min. The detector temperature was set at 275 °C and the injection port at 200 °C. The flow rates for the gases were as follows: helium (12 mL/min.); hydrogen (40 mL/min.); and zero air (460 mL/min.). Standards were prepared by adding *cis*-DCE dissolved in methanol and VC, ethene, and methane gases, all at known volumes, to a serum bottle (70 mL) containing deionized water (5 mL). Nominal aqueous phase detection limits for *cis*-DCE and VC were 200 and 50 μg/L, respectively.

Acetate, propionate, and pyruvate were quantified by direct injection of aqueous samples onto a GC (Hewlett-

Packard 5890) equipped with a FID and a packed column (6 ft. x $^1/_8$ in. OD) containing 80/100 Porapak QS (Alltech). During the run the oven was isothermal (190 °C), and the injection port and detector temperatures were maintained at 215 and 225 °C, respectively. Gas flow rates were as follows: helium (20 mL/min.); hydrogen (40 mL/min.); and zero air (480 mL/min.). All samples were filtered (0.5 μm) during sampling and were acidified with 50% H$_2$SO$_4$ (20 μL/mL) prior to injection onto the GC. Standards were prepared gravimetrically in deionized water and then diluted to the desired concentrations in separate vials with deionized water. Standards were run daily and acidified before injection.

Radiolabeled ^{14}C ethenes were measured daily by adding aqueous samples (5 mL) to scintillation vials (20 mL) containing scintillation cocktail (10 mL) and run after a period not less than 24 h in a scintillation counter (Beckman LS 6500). Blanks containing only the scintillation cocktail were always counted in conjunction with the samples for correction purposes.

Determination of Partition Coefficients. Tridecane/water partition coefficients (K_i^{o-w}) with units of ($L-tridecane/L-water$) for PCE, TCE, and *cis*-DCE were previously determined by Carr et al. (*19*). The tridecane/water partition coefficient for VC was determined by contacting deionized water (20 mL) with a VC/N$_2$ headspace in a serum bottle (160 mL). The system was allowed to equilibrate, and the dissolved VC solution was divided into two bottles, the first being a control (5 mL) used to quantify the initial VC concentration using GC headspace analysis, and the second sample (15 mL) was added to a serum bottle (15 mL) that had been capped with a Teflon-lined butyl rubber septum and aluminum crimp cap. After sealing the bottle, tridecane (1 mL) was added displacing an equal aqueous volume. Samples were then placed on a shaker table at room temperature (24 °C $\pm$ 0.57) for a period of at least 24 h. Following equilibration between the two phases, an aqueous sample (5 mL) was analyzed for VC by headspace sampling on a GC. The difference between the control and the water in the NAPL-system allowed for the determination of the VC tridecane/water partition coefficient.

Column Design. Experiments were carried out in columns as depicted in Figure 1. Columns were glass (25 cm $\times$ 2.5 cm

TABLE 1. Information on Condition of Individual Columns

	column		
	low donor concn (LDC)	intermediate donor concn (IDC)	high donor concn (HDC)
column volume (mL)	167.0	150.6	150.0
pore volume (mL)	60.6	54.4	53.4
porosity	0.36	0.36	0.36
flow rate (mL/h)	0.842	0.756	0.742
residual NAPL (%)	16.3	14.6	12.5
pyruvate concn (mM)	25	100	250

ID, Spectrum Chromotography) with stainless steel endpieces fitted with screens (Rice University Support Shop) attached to each end with a threaded polymer collar and sealed with viton O-rings (American Packing and Gasket Co.). Each endpiece accepted Swagelok fittings to allow connection of both Teflon tubing and a glass sampling port with Teflon stopcock (Rice University Support Shop) to the column.

Each column was packed to capacity with $500-750$ μm diameter glass beads (Polysciences, Inc.) in an alternating fashion between the addition of glass beads (1 cm thick lifts) and the introduction of deionized water to fill the pore spaces. A rubber mallet was employed to vibrate the column after each lift of beads was added, yielding consistent final porosities of 0.36. Each column had slightly different total volumes and corresponding pore volumes, but individual flow rates were adjusted to yield a retention time of 3 days (see Table 1).

NAPL Preparation. A mixture of tridecane and labeled ^{14}C-PCE was prepared to simulate a PCE-containing NAPL that consisted of an insoluble and recalcitrant organic fraction—very similar to the formulated NAPL used in previous studies (*19*). PCE, which contained a ratio of unlabeled and ^{14}C fractions of 94 to 1, was dissolved in tridecane to a final weight fraction of 0.12 g PCE/g NAPL (0.13 mol PCE/mol NAPL, based on an average molecular weight of 182 g/mol). The NAPL was dyed to a visually distinguishable red tone with Sudan III to make mobilized NAPL product detectable. The density of the NAPL was 0.81 g/mL, and the specific activity was 6.23×10^5 DPM/mL.

NAPL Flooding/Flushing and Start-Up. After column packing was complete, NAPL was added to each column in a downflow manner in order to avoid gravitational fingering. NAPL (approximately 50 mL) was added through Teflon tubing that extended from the top of column that was affixed to a glass-barreled syringe (50 mL) with Teflon plunger (Supelco). The Teflon tubing at the bottom of the column connected to a separatory funnel for collection and separation of the deionized water and NAPL. The influent NAPL was pumped at a rate of 1 mL/min., (Harvard Apparatus syringe pump, Model 22) through the column, and the NAPL was visually tracked until it exited the column from the effluent tubing.

To obtain a residual NAPL, the flooding was followed by deionized water flushing to mobilize free NAPL. The flushing was carried out in an upflow manner to achieve uniform flow through the column and to minimize channeling. Each column was flushed with DI water (10 pore volumes) at progressively lower flow rates (pore volumes 1–4 at 4.0 mL/min.; pore volumes 5–8 at 2.0 mL/min.; pore volumes 9–10 at 1.0 mL/min.) until no NAPL was observed exiting the column. The contents of the separatory funnel readily separated and were quantified gravimetrically.

Each column was left undisturbed overnight (12 h with no flow) to allow for potential NAPL redistribution prior to the microbial inoculation. The inoculum consisted of a mixed culture of dechlorinating and methanogenic bacteria that

has been used in previous studies (*16*). Three pore volumes of the inoculum were introduced to the column in the same manner as the DI flushing at flow rates of 4.0, 2.0, and 1.0 mL/min. for the first, second, and third pore volumes, respectively. Small volumes of NAPL were mobilized during the inoculation and again gravimetrically quantified. Once the inoculation was complete the nutrient medium flow, which had been separated between two syringes to eliminate in-syringe fermentation, was started. One syringe contained only electron donor (pyruvate) in deionized water, while the other contained the remainder of the nutrients and sodium bicarbonate buffer in deionized water.

Protocol for Column Experiments. Three biotic columns were run concurrently—each with identical operating parameters but for the concentration of electron donor and sodium bicarbonate in the nutrient medium. Pyruvate concentrations were 25, 100, and 250 mmol in the nutrient medium for columns low donor concentration (LDC), intermediate donor concentration (IDC), and high donor concentration (HDC), respectively. Sampling commenced 1 day after the introduction of the medium. Samples (5 mL), for ^{14}C analysis, were collected daily, while chlorinated ethenes and organic acids were sampled every 3 days (one sample for each pore volume throughput). Daily pH measurements of column effluents were made, and sodium bicarbonate concentrations were adjusted to attain a similar range of pH in all columns. All samples were drawn from the glass sampling port on the top of the column using a stainless steel needle (Popper, 6 in., 22 gauge) and gastight syringe (Hamilton 250 μL locking or Hamilton 10 mL). Each column had dedicated sampling instruments that were rinsed in methanol and deionized water after every use. Nutrient medium was refreshed every 6 days by exchanging empty syringes with new, full syringes (B–D, 60 mL). To prevent backflow during the exchange the two-way valve at the bottom of the column was closed until the syringes with new media were in place.

During the first 2 weeks of operation small NAPL globules were observed in column effluent. The red globules were easily detected visually, and the phases were separated in the separatory funnel. NAPL volumes were gravimetrically quantified and residual saturation values updated based on the NAPL loss.

Trapped Gas Measurements. After 75 days of operation, the influent medium was replaced with NaOH (1 N) to halt biological activity and to provide an estimate of the volume of carbon dioxide gas trapped in each column. Flow rates remained the same as those maintained during the experiment. Three days were allowed for one complete pore volume of sodium hydroxide to be pumped into the column. The difference between the volume added to the column and volume removed from the column during this period was assumed to be approximately equal to the volume of carbon dioxide gas trapped in each column at the experiments endpoint.

Column Dissection. Each column was subjected to cryogenic dissection following the sodium hydroxide flush, in an attempt to gain an understanding of dechlorination and dissolution patterns. Columns were dissected into three equal pieces: top, middle, and bottom (each ~ 8.3 cm long). First the aqueous phase from the column was drained and sampled to ensure that the NAPL had remained trapped in the pore spaces of the column. After draining the aqueous volume each endpiece was capped with a Swagelok plug fitting, and stainless steel pipe clamps were attached at locations along each column to provide resistance against expansion during freezing. The columns were delineated into sections of equal length and then placed in a freezer (-20 °C) for a period of not less than 24 h. The frozen columns were scored at the indicated marks and broken using a

fulcrum and hand-pressure. The column section was then immediately placed into a sampling jar (Qorpak, 16 oz.) partially filled with Tridecane (100 mL), sealed with a Teflon-lined lid, and placed in a freezer. After all the dissections were complete, jars were allowed to warm to room temperature. Samples were thoroughly mixed to ensure complete dissolution of the residual NAPL into the much larger volume of tridecane solvent.

Measurement of Activity and Chlorinated Concentrations by Section. The chlorinated ethenes were quantified by gravimetric sampling of tridecane from each jar with ^{14}C activity counts made with the method outlined previously. To determine the distribution of the various chlorinated ethenes, deionized water (15 mL) was added to a serum bottle (15 mL) followed by the addition of a tridecane sample from each column sample jar (5 mL) to displace an equal volume of deionized water resulting in a volumetric ratio of 2:1 between the aqueous and tridecane phases. Serum bottles were placed on a shaker table at room temperature for a period of 12 h. Aqueous phase samples were analyzed by GC to quantify chlorinated ethenes. Partition coefficients were then used to compute the mass of each constituent in a particular column section.

Results

Determination of Partition Coefficients. Dimensionless partition coefficients for PCE, TCE, and *cis*-DCE were previously determined experimentally by Carr et al. (*19*). The results reported were as follows: $K_{PCE}^{o-w} = 3060$; $K_{TCE}^{o-w} = 395$; and $K_{DCE}^{o-w} = 94$. In this study the VC tridecane partition coefficient was determined experimentally and found to be $K_{VC}^{o-w} = 4.0$.

Column Experiments. *Gas Production and pH.* Gas production in each column commenced shortly after inoculation. Small gas bubbles collected and became trapped in the pore spaces, visible through the glass column walls. However, dissolved effluent methane concentrations remained near zero throughout the experiment for all columns, indicating that the gas was primarily carbon dioxide. Estimates of the volumes of trapped CO_2 in each column roughly correlated to the amount of electron donor added to each system. Columns LDC, IDC, and HDC contained approximate gas volumes of 4.0, 11.5, and 14.5 mL, respectively. These volumes relate to pore volume percentage as follows: LDC (7% of pore volume), IDC (21% of pore volume), and HDC (27% of pore volume). Increasing gas volumes yielded higher seepage velocities than calculated assuming a two-phase system (aqueous/NAPL) absent of any residual gas phase. Daily effluent pH measurements fell within the range of 6.3−6.9 for all columns over the entire experimental period.

Organic Acids. Influent pyruvate was partially or fully fermented to propionate and/or acetate for all columns as seen in Figure 2. Complete conversion of pyruvate to acetate and propionate was achieved from the outset in columns LDC and IDC. Over the course of the experiment column LDC had effluent electron donor concentrations that were predominately acetate (91%) with the balance present as propionate. A similar comparison of column IDC shows that pyruvate was fermented to acetate (78%) and propionate (22%), with no measurable pyruvate in the effluent. A different pattern was observed for column HDC which had a microbial community that continued to improve its fermentation extent and rate over the experimental period. For the first half of the experiment approximately half of the influent pyruvate was exiting the column unfermented with the balance exiting as acetate. By day 38, increased activity led to effluent organic acid concentrations increasingly dominated by acetate and propionate (which had not been measured above trace levels
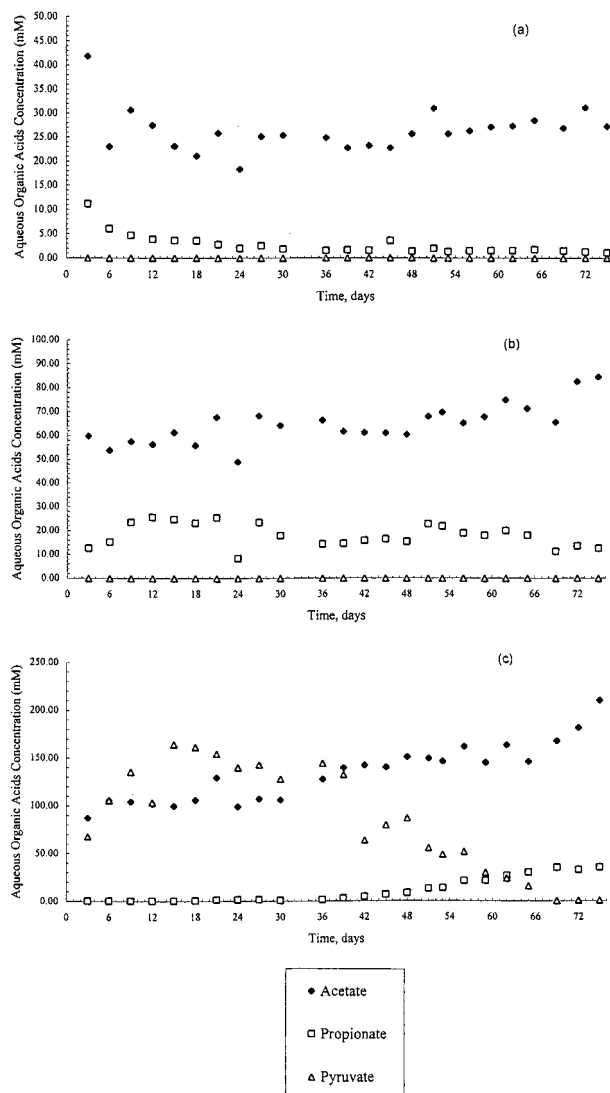

FIGURE 2. Temporal aqueous phase organic acid concentrations: (a) column LDC, (b) column IDC, and (c) column HDC. The following symbols are consistent in all panels: acetate (♦), propionate (□), and pyruvate (△).

before day 36). By the end of the experiment, effluent electron donor was composed of acetate (85%) and propionate (14%) with only trace levels of pyruvate remaining.

Chlorinated Ethenes. The chlorinated ethenes concentrations from effluent samples are presented in Figure 3. Extensive dechlorination began at the outset of the experiment in two of the three columns. However, the quantity and extent of halorespiration did not correspond to the quantity of electron donor added to each system. In all cases dechlorination ceased with the production of VC; ethene was not observed in any of the systems.

Results from column LDC are presented in Figure 3a. Relatively large quantities of VC were present in the column effluent through day 27. These substantial VC concentrations observed early in the experiment were not sustained, exhibiting a rapid tailing following the maximum concentration on day 24. Accompanying the decline in VC concentration was a gradual increase in effluent TCE concentration until the experiments' endpoint. Higher *cis*-DCE concentrations were also observed starting at day 34, peaking at day 45, then falling slightly, and remaining nearly constant for the final 21 days. PCE concentrations remained near the predicted equilibrium value over the entire experimental period.
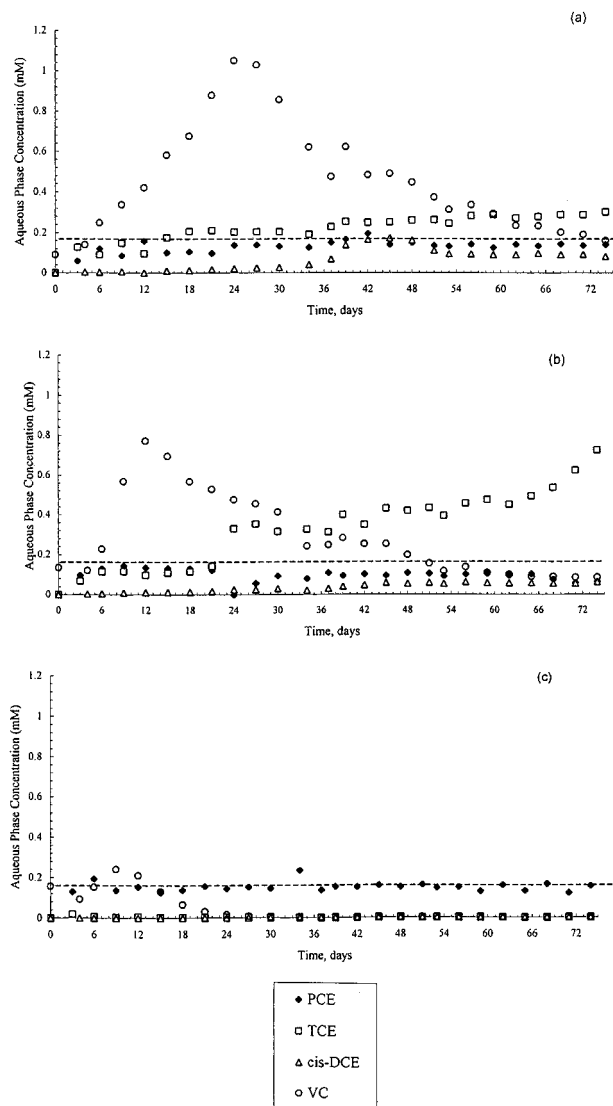
FIGURE 3. Temporal aqueous phase chlorinated ethene concentrations: (a) column LDC, (b) column IDC, and (c) column HDC. The following symbols are consistent in all panels: PCE (◆), TCE (□), cis-DCE (△), and VC (○) and the dashed line represents the calculated aqueous solubility of PCE exiting columns without any dechlorination.

The data for column IDC are shown in Figure 3b and are similar to column LDC data for the initial 2-week period but exhibit a more rapid decline in VC production. A pronounced change in the effluent chlorinated ethenes occurred at day 24; TCE concentration more than doubled from the previous sampling, and PCE was virtually absent in the sample. Following this change, PCE concentrations increased to levels about half that expected from equilibrium dissolution alone and remained so from day 30 to 75. TCE concentrations continued to increase from day 24 to the end of the experimental period with the highest concentration measured at the final sampling—day 75. The production of cis-DCE was lower than that observed in column LDC and was consistent throughout the second half of the experiment (days 38—75).

Much different results were observed for column HDC as can be seen in Figure 3c. With the exception of limited VC production early in the study, the only observed removal was due to PCE dissolution. The concentrations of PCE remained near the theoretical equilibrium prediction (dashed line) for the entire experiment.
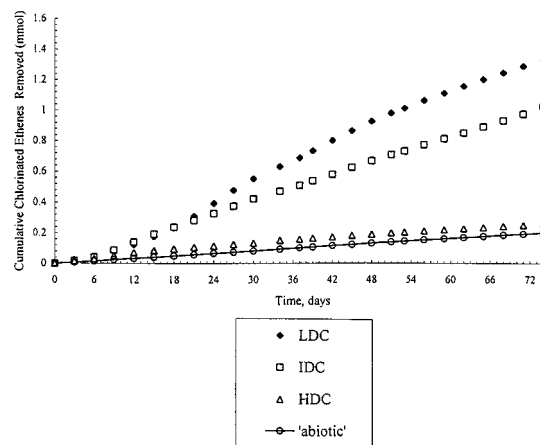

FIGURE 4. Cumulative moles of chlorinated ethenes collected from all three columns LDC (◆), IDC (□), HDC (△), and removal based on PCE dissolution only (○).

TABLE 2. Final Chlorinated Ethenes Mass Balance by ^{14}C Analysis

	column		
	LDC (%)	IDC (%)	HDC (%)
^{14}C NAPL removed (flushing)[a]	82	85	86
^{14}C removed (effluent)[b]	5	4	1
^{14}C remaining	11	9	12
mass balance	98	97	99

[a] Removal during the initial deionized water flushing plus NAPL removed during the first two experimental weeks. [b] Dissolved chlorinated ethenes, equal to the cumulative removal.

Cumulative chlorinated ethenes removed from all columns are displayed in Figure 4. Significantly enhanced removal was achieved in columns LDC and IDC. Column HDC was just slightly more effective than removal by dissolution alone despite the large quantities of electron donor added to the system. The cumulative flux of chlorinated ethenes removed from column LDC and IDC was far greater than PCE dissolution under abiotic conditions, with enhancement factors (total moles of removal divided by moles of removal due to PCE equilibrium dissolution only) of 6.5 and 5.0, respectively. The enhancement factor for column HDC was only slightly greater than unity at 1.3.

Column Dissection. Results of ^{14}C mass balances, completed after analyzing column sections, are presented in Table 2. Each section was also analyzed to determine the chlorinated constituents distribution within the columns. The column sections were analyzed for total ^{14}C and to determine the relative fractions of PCE and TCE in each section. These data is shown in Table 3. The remaining chlorinated ethenes were either not present or at too low a concentration for the GC techniques employed. If present, their low concentrations would make them only trace contributors to the total chlorinated solvent mass remaining in the systems.

Each column exhibited different trends that may have been influenced by several variables including both biological and physical/chemical factors. As can be seen from the data in Table 3, column LDC had a distribution of chlorinated ethenes that was highest toward the bottom of the column. TCE concentrations were highest at the column base, and overall more than $^{1}/_{3}$ of the total chlorinated ethenes (added as PCE) remaining in the column had been reduced to TCE. Column HDC also exhibited the highest concentration of ^{14}C ethenes in the bottom section, although no TCE was detected in the column. A much different pattern was evidenced in column IDC. In this case the bottom section was the most

TABLE 3. Column Chlorinated Ethenes by Section

	LDC			IDC			HDC		
section	top	middle	bottom	top	middle	bottom	top	middle	bottom
^{14}C fraction	0.25	0.35	0.40	0.34	0.48	0.18	0.21	0.24	0.55
fraction as PCE	0.79	0.70	0.59	0.41	0.05	0.20	1.00	1.00	1.00
fraction as TCE	0.21	0.30	0.41	0.59	0.95	0.80	0.00	0.00	0.00

depleted section in the column. A majority of the ^{14}C ethenes and chlorinated mass was contained in the middle column section with significant quantities also residing in the top third of the column. At the end of the 75-day experimental period almost 80% of the remaining chlorinated ethenes dissolved in the NAPL was TCE.

Discussion

The objective of this research was to determine the effect of dechlorinating bacteria on the fate of PCE and its reduced products in the presence of PCE-containing NAPLs in column systems. The determination of the final tridecane/water partition coefficient of VC was important for understanding the compositional changes in the NAPL over the experimental period. Partition coefficients decrease as the chlorinated ethenes became more reduced, corresponding to an increase in their aqueous solubility. A result of this behavior is an increased removal rate from a source zone for more reduced chlorinated ethenes relative to PCE. Hence, total removal of chlorinated ethenes is strongly dependent not only on the rate of dechlorination but the extent as well.

Column experiments were designed to quantitatively describe the effect of dechlorination on the removal of chlorinated ethenes from a NAPL source zone compared to theoretical dissolution alone. The experimental design simulated a medium-to-coarse grained sand aquifer with a groundwater velocity of 8 cm/day, containing a residual NAPL. The NAPL used for these studies consisted of labeled ^{14}C-PCE and a conservative hydrocarbon to imitate a mixed organic waste, very similar to that used by Carr et al. (*19*). This composition was chosen based on the observation that many chlorinated solvent spills occur in the presence of fuels or other organics (*2, 5, 30*). The large mass of insoluble tridecane served to create a NAPL that would undergo only minor volumetric reductions over the course of the experiment—serving to reduce the potential for NAPL redistribution that might be expected following volumetric losses.

Early gas production in all three columns indicated biologically active systems. Collection of gas in the pore spaces reduced the effective volume of each column, most severely impacting column HDC. The reduction in available pore space did not appear to inhibit the contact between the microbes in the aqueous phase and the chlorinated ethenes. It did, however, serve to increase the flow velocity through the columns. Methane was detected only at low-levels indicating that methanogenic activity was not competing significantly with the dechlorinating bacteria for available hydrogen. Effluent pH for all columns was lower than that observed in the inoculum culture, but it was generally within the viable range for dechlorinating bacteria (pH 6.4−7.2). The only aberration from this range was column HDC that had pH values near 6.3 for the first 2 weeks of the experiment.

Organic acids data indicate that proper growth conditions for the fermenting bacteria were present in all columns. The balance between the influent organic acid (pyruvate) and the effluent acids (acetate, propionate, pyruvate) show that on average 91% of the influent organic acid was measured in the effluent (mol/mol). Some loss of carbon is expected for incorporation into cells, thus it appears that acetate was not likely an electron donor for dechlorination activity, as has been observed by others (*6, 8−10*). Further support of

$$[C_3H_3O_3^- + 5 \cdot H_2O \leftrightarrow 2 \cdot CO_2 + 5 \cdot H_2] \qquad \text{pyruvate} \quad (I)$$
$$\text{fermentation products}$$
$$[7 \cdot H_2 + 2 \cdot CO_2 \leftrightarrow C_3H_5O_2^- + 5 \cdot H_2O] \cdot (y) \qquad \text{propionate} \quad (II)$$
$$[4 \cdot H_2 + CO_2 \leftrightarrow C_2H_3O_2^- + 3 \cdot H_2O] \cdot (1-y) \qquad \text{acetate} \quad (III)$$

$$C_3H_3O_3^- + [5-(2y+3)] \cdot H2O \leftrightarrow (y)C_3H_5O_2^- + (1-y)C_2H_3O_2^- + [5-(3y+4)] \cdot H_2 + [2-(y+1)] \cdot CO_2 \quad (IV)$$

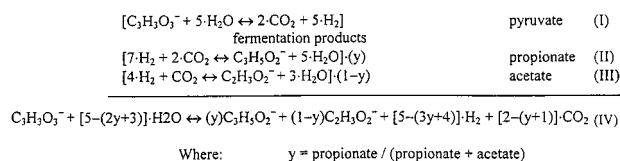Where: $y = $ propionate / (propionate + acetate)

FIGURE 5. Equation developed to calculate hydrogen production based on the fraction of propionate produced (y). The equation assumes no microbial growth and reflects observations of no hydrogen consumption by hydrogenotrophic bacteria.

TABLE 4. Calculated Hydrogen Yield as a Fraction of Organic Acids Formed

propionate fraction (y)	acetate fraction ($1-y$)	hydrogen yield (mmol/mmol pyruvate)
0.00	1.00	1.00
0.10	0.90	0.70
0.20	0.80	0.40
0.30	0.70	0.10
0.40	0.60	−0.20
0.50	0.50	−0.50
0.60	0.40	−0.80
0.70	0.30	−1.10
0.80	0.20	−1.40
0.90	0.10	−1.70
1.00	0.00	−2.00

this observation comes from studies involving this particular culture (data not shown) that have confirmed that acetate does not support dechlorination activity (*31*). In fact, effluent acetate concentrations in column LDC were often greater than the influent pyruvate (mol/mol) suggesting that an active acetogenic population was present. The behavior of column HDC indicates that the initial population of active fermenting organisms could not fully utilize the influent pyruvate, and much of what was in the feed simply washed out of the column. Over the course of the experiment the fermentative population became more robust, and by day 70, pyruvate was completely absent in the effluent.

Analysis of the organic acids data provides information on estimating hydrogen generation using the equations shown in Figure 5. The combined equations for pyruvate conversion to propionate and acetate yielded a single equation (eq IV) that was used to calculate the quantity of hydrogen produced in each system using only the organic acids data and influent electron donor concentrations. Equation IV rests on the assumption that all pyruvate is fermented to either acetate or propionate in the absence of methanogenesis (this is not rigorously correct as it neglects growth). Total hydrogen production is obtained from the product of hydrogen yield from eq IV (mol/mol pyruvate) and the concentration of influent pyruvate in the nutrient medium. To correct for incomplete fermentation of the influent pyruvate in column HDC, the concentration was scaled to equal the pyruvate added minus the concentration of that measured in the effluent. As can be seen in Table 4 the distribution of fermentation products is extremely important to the available hydrogen in the system. When the fraction of fermentation products becomes greater than $^1/_3$ propionate, the system will actually require hydrogen inputs

rather than produce hydrogen to be used in reductive dechlorination.

Each of the three columns produced significant amounts of hydrogen from the fermentation of the influent pyruvate. Predictions over the 75-day experiment showed that columns LDC, IDC, and HDC produced 28, 49, and 163 mmol of hydrogen, respectively. Methanogenesis was not a significant competitor for the hydrogen, so a majority of the hydrogen produced was presumably "available" for dechlorination.

Dechlorination was observed in all columns during the initial 10-day period, but the activity continued only in columns LDC and IDC after that time. Based on observed extents of dechlorination it appears that all three columns experienced some washout of dechlorinating organisms over the course of the experiment. Column HDC was most severely affected, with washout removing essentially the entire dechlorinating population early in the experiment. Both columns LDC and IDC appear to have washed out a majority of the cis-DCE degrading organisms by the midpoint of the experiment (day 38) while retaining the organism(s) responsible for PCE and TCE dechlorination. This result is not surprising based on the slow growth rates of cis-DCE degraders that have been observed in highly purified enrichment cultures in our laboratory (31). The timing of the washout of cis-DCE degraders was crucial to cumulative ethenes removal—primarily due to the high concentrations of VC that were produced and the significantly lower partition coefficient of VC compared to the other chlorinated ethenes. The more rapid washout of the dechlorinating organisms in columns IDC (cis-DCE degraders) and HDC (all dechlorinators) appears to be related to the CO_2 production and retention within the columns. The increase in flow velocity for columns IDC and HDC was 21% and 26%, respectively; compared with an increase of less than 10% for column LDC. The significantly different behavior of the columns IDC and HDC may also be a result of slight pH differences observed early in the experiment that may have yielded less than optimal growth conditions in column HDC.

Data of total chlorinated ethenes removal indicates that column LDC achieved the highest removal levels in effluent samples over the 75-day experiment. Column IDC also exhibited removal of chlorinated ethenes that was far above that from PCE-dissolution alone. Interestingly, a longer experimental period would likely have shown even greater enhancement in column IDC. By the end of the study, the effluent contained elevated concentrations of TCE, evidence of a NAPL that was considerably enriched with TCE. High aqueous TCE concentrations have the potential to select for cis-DCE production, which in turn would have greatly enhanced the rate of source depletion.

Column dissection results supported this theory, indicating that column IDC had depleted a majority of its PCE. The bulk of the initial PCE remained in the NAPL in the form of TCE. As TCE was transported in the column, it was retained in the NAPL due to its high partition coefficient. Column effluent data did not reflect this large production of TCE until all of the NAPL, extending from the zone of dechlorination at the base through the top of the column, developed elevated TCE levels capable of yielding the high effluent aqueous phase concentrations observed by the end of the experiment.

Information gathered in the column dissection studies suggests that significant spatial variations existed in dechlorination pattern among columns. Column LDC appears to have dechlorinated primarily from the top of the column, perhaps progressing down the column over the course of the experiment, whereas column IDC depleted the bottom section of PCE initially and had a large mass of TCE migrating upward with the flow of fresh nutrient medium entering the base. Unfortunately, the spatial and temporal variability in

dechlorination made biomass determinations and kinetic analysis unreliable, and dissection of the columns provided data only on the total reduction of PCE to the various less-chlorinated ethenes.

Calculating efficiency (the fraction of hydrogen used for dechlorination in relation to the predicted total hydrogen production) as a gauge of performance for each column was conducted using calculated hydrogen production and measured total PCE reduction. Hydrogen use efficiency calculations for columns LDC, IDC, and HDC were 13%, 7.0%, and 0.1%, respectively. The observed efficiency decrease that accompanied increasing influent pyruvate concentrations occurred as expected, particularly for column HDC which exhibited almost no dechlorination activity.

Despite the more efficient performance of column LDC with regard to hydrogen utilization, the fraction of chlorinated ethenes remaining in the NAPL was predominately PCE (68%) with the balance as TCE. Column IDC, alternatively, had lower hydrogen use efficiencies, but PCE accounted for only 20% of the remaining NAPL chlorinated ethenes, again with the balance as TCE. The conversion of PCE to TCE results in a partition coefficient reduction that decreases the longevity of the contaminant by nearly 8-fold. In the worst case scenario where dechlorination ceased after 75 days complete chlorinated ethene dissolution would have been achieved (assuming no mass transfer resistances) in 617 days, 158 days, and 1135 days for columns LDC, IDC, and HDC, respectively. This may indicate benefits to adding an amount of electron donor far beyond stoichiometric requirements, at the expense of efficient hydrogen use, although it may be possible (based on results from column HDC) to add detrimental levels of electron donor.

Column studies demonstrated that dechlorinating bacteria could significantly impact the longevity of PCE-containing NAPL source zones. The reduction of PCE to less chlorinated ethenes greatly increases the aqueous solubility of the contaminants in conjunction with increasing the overall mass-transfer of PCE to the aqueous phase. As shown by Carr et al. (19), the partitioning behavior of the terminal chlorinated ethene was essential in evaluating the longevity of the chlorinated ethene fraction of the NAPL. Longevity of a source zone will be diminished by greater extents of dechlorination; however, the heterogeneous nature of the NAPL within the columns resulted in effluent analysis that yielded only information representative of NAPL/water equilibrium at the exit of the column. Thus, effluent samples did not reflect significant amounts of PCE reduction taking place, which could only be confirmed by the final destructive sampling. Cumulative removal of all chlorinated ethenes from the columns was not correlated to the influent pyruvate concentration, and if the observed results are accurate it appears that it may be possible to add excessive levels of electron donor. Efficient use of electron donor has been the subject of much interest in plume-remediation where the volumes of water to be treated are much larger, and amendment costs are important in evaluating the economic viability. The smaller volume of source zones compared to plumes—and the potential cost-savings realized by reducing the time a remediation system needs to operate after a source is exhausted of contamination—may make efficiency criteria less important. Ultimately, the tradeoffs between substrate costs and the remediation operation time frame need to be analyzed, with the best solution optimizing the two parameters to obtain a cleanup strategy offering the largest net benefit/cost ratio. The ability of dechlorinaters to grow at high aqueous concentrations (even at saturation) of PCE, coupled with results from this study, suggest that such analysis be conducted to evaluate the viability of source zone bioremediation as a strategy to reduce the duration of long-term NAPL problems.

Literature Cited

(1) 1)McCarty, P. L. *Curr. Opinions Biotechnol.* **1993**, *4*, 323−330.
(2) EPA. *Evaluation of the Likelihood of DNAPL Presence at NPL Sites, National Results*; U.S. Environmental Protection Agency, Office of Solid Waste and Emergency Response: 1993.
(3) Pankow, J. F.; Cherry, J. A. *Dense Chlorinated Solvents and Other DNAPLs in Groundwater*; Waterloo Press: Portland, 1996.
(4) Bedient, P. B.; Rifai, H. S.; Newell, C. J.; Wilson, J. T. *Groundwater Contamination: Transport and Remediation*, 2nd ed.; Prentice Hall, Inc.: Upper Saddle River, NJ, 1999.
(5) Wiedemeier, T. H.; Rifai, H. S.; Newell, C. J.; Wilson, J. T. *Natural Attenuation of Fuels and Chlorinated Solvents in the Subsurface*; John Wiley & Sons: New York, 1999.
(6) Bouwer, E. J.; McCarty, P. L. *Appl. Environ. Microbiol.* **1983**, *45*, 1286−1294.
(7) Parsons, F.; Wood, P. R.; DeMarco, J. *J. Am. Water Works Assoc.* **1984**, *76*, 56−59.
(8) Vogel, T.; McCarty, P. *Appl. Environ. Microbiol.* **1985**, *49*, 1080−1083.
(9) Fathepure, B.; Boyd, S. A. *Appl. Environ. Microbiol.* **1988**, *54*, 2976−2980.
(10) Freedman, D. L.; Gossett, J. M. *Appl. Environ. Microbiol.* **1989**, *55*, 2144−2151.
(11) DiStefano, T. D.; Gossett, J. M.; Zinder, S. H. *Appl. Environ. Microbiol.* **1991**, *57*, 2287−2292.
(12) deBruin, W. P.; Kotterman, M. J. J.; Posthumus, M. A.; Schraa, G.; Zehnder, A. J. B. *Appl. Environ. Microbiol.* **1992**, *58*, 1996−2000.
(13) DiStefano, T. D.; Gossett, J. M.; Zinder, S. H. *Appl. Environ. Microbiol.* **1992**, *58*, 3622−3629.
(14) Ballapragada, B. S.; Stensel, H. D.; Puhakka, J. A.; Ferguson, J. F. *Environ. Sci. Technol.* **1997**, *31*, 1728−1734.
(15) Fennell, D. E.; Gossett, J. A.; Zinder, S. H. *Environ. Sci. Technol.* **1997**, *31*, 918−926.
(16) Carr, C. S.; Hughes, J. B. *Environ. Sci. Technol.* **1998**, *32*, 1817−1824.
(17) Lee, M. D.; Quinton, G. E.; Beeman, R. E.; Biehle, A. A.; Liddle, R. L.; Ellis, D. E.; Buchanan, R. J. *J. Ind. Microbiol. Biotechnol.* **1997**, *18*, 106−115.
(18) Lee, M. D.; Odom, J. M.; Buchanan, R. J. *Annu. Rev. Microbiol.* **1998**, *52*, 423−452.
(19) Carr, C. S.; Garg, S.; Hughes, J. B. *Environ. Sci. Technol.* **2000**, *34*, 1088−1094.
(20) Yang, Y.; McCarty, P. L. *Environ. Sci. Technol.* **2000**, *34*, 2979−2984.
(21) Sharma, P. K.; McCarty, P. L. *Appl. Environ. Microbiol.* **1996**, *62*, 761−765.
(22) Isalou, M.; Sleep, B. E.; Liss, S. N. *Environ. Sci. Technol.* **1998**, *32*, 3579−3585.
(23) Nielsen, R. B.; Keasling, J. D. *Biotechnol. Bioeng.* **1999**, *62*, 160−165.
(24) Holliger, C.; Schraa, G.; Stams, A. J. M.; Zehnder, A. J. B. *Appl. Environ. Microbiol.* **1993**, *59*, 2991−2997.
(25) Holliger, C.; Hahn, D.; Harmsen, H.; Ludwig, W.; Schumacher, W.; Tindall, B.; Vazquez, F.; Weiss, N.; Zehnder, A. J. B. *Arch. Microbiol.* **1998**, *169*, 313−321.
(26) Neumann, A.; Scholz-Muramatsu, H.; Diekert, G. *Arch. Microbiol.* **1994**, *162*, 295−301.
(27) Scholz-Muramatsu, H.; Neumann, A.; MeBmer, M.; Moore, E.; Diekert, G. *Arch. Microbiol.* **1995**, *163*, 48−56.
(28) Seagren, E. A.; Rittmann, B. E.; Valocchi, A. J. *J. Contam. Hydrol.* **1993**, *12*, 103−132.
(29) Seagren, E. A.; Rittman, B. E.; Valocchi, A. J. *Environ. Sci. Technol.* **1994**, *28*, 833−839.
(30) Nyer, E. K. *Ground Water Monitoring Rev.* **1999**, *Winter*, 62−66.
(31) Carr, C. S. Ph.D. Dissertation, Department of Environmental Science and Engineering, Rice University, Houston, TX, 2000.